NASA Technical Memorandum 4161

A Statistical Study of the Surface Accuracy of a Planar Truss Beam

W. Scott Kenner and W. B. Fichter

FEBRUARY 1990

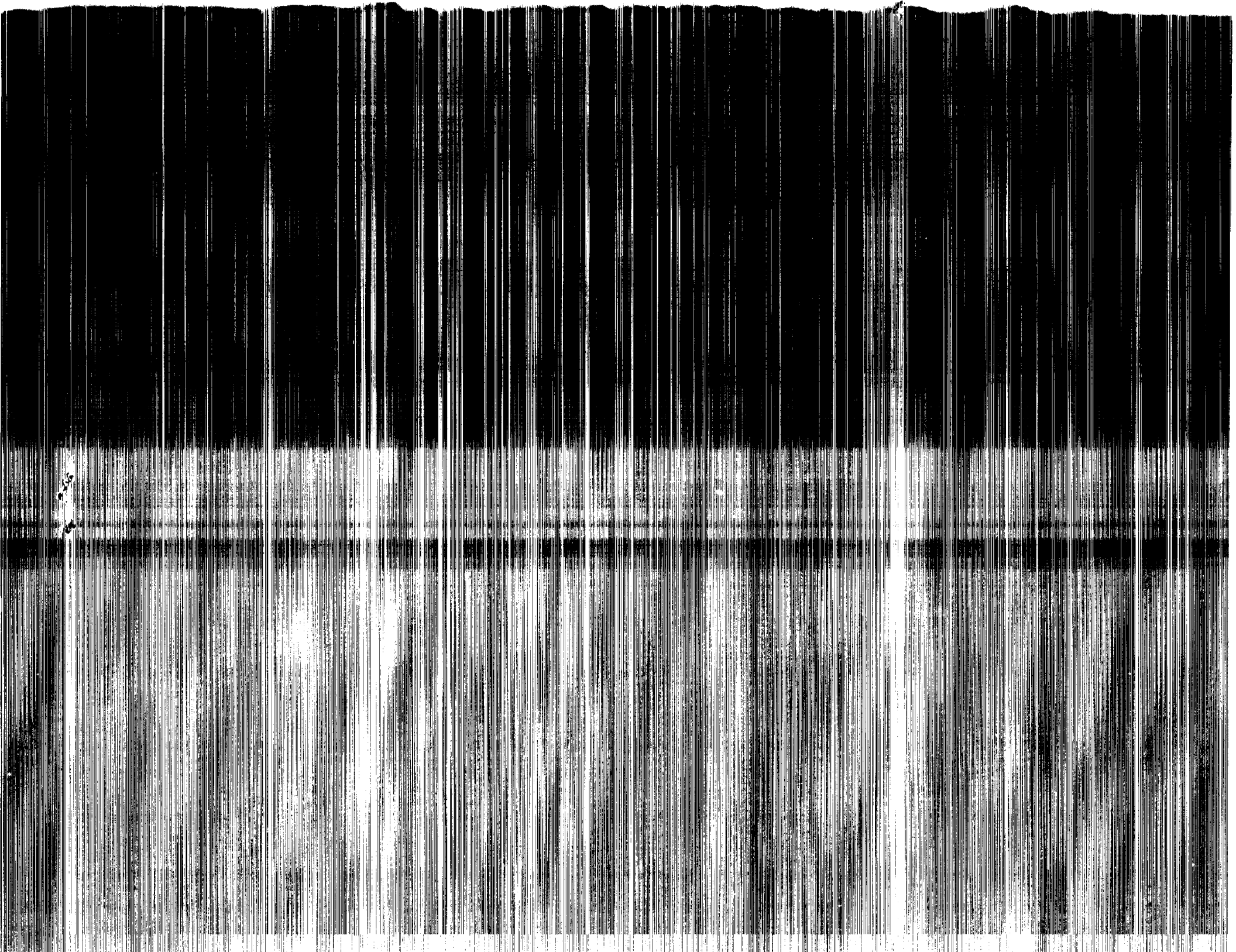

NASA Technical Memorandum 4161

A Statistical Study of the Surface Accuracy of a Planar Truss Beam

W. Scott Kenner and W. B. Fichter
Langley Research Center
Hampton, Virginia

National Aeronautics and
Space Administration
Office of Management
Scientific and Technical
Information Division

1990

Summary

Surface error statistics for one statically determinate and two statically indeterminate planar truss beams with random member-length errors were calculated using a Monte Carlo technique in conjunction with finite-element analysis. Surface error was calculated in terms of the normal distance from a regression line to the surface nodes of the distorted beam. Results for both single-layer and double-layer truss beams indicate that there exists a minimum root-mean-square surface error that depends on the depth-to-length ratio of the beam. Results also indicate that double-layer beams can provide greater surface accuracy than single-layer beams, though at the cost of a disproportionately large number of additional members.

Introduction

Many future space platforms and reflectors will require stable and accurate support structures. (See, for example, ref. 1.) Trusses are good candidates for many of these support structures because they are lightweight and stiff, and their static response is predictable. Also, when carefully manufactured and assembled, they have the potential for achieving accurate surfaces. Among the factors that can influence the surface accuracy of trusses are manufacturing tolerances and uncertainties in coefficient of thermal expansion, both of which can reasonably be treated as random variables. Therefore, studies of trusses under the influence of random imperfections should provide useful information on the design and fabrication of many space structures that require accurate surfaces.

Planar truss beams are of interest because they have some of the structural characteristics of three-dimensional trusses but their analysis involves less computational complexity. Some previous analyses of statically determinate single-layer truss beams with random member-length errors are presented in references 2 and 3. In reference 2, a continuum model of a statically determinate truss beam was employed to analyze the effect of zero-mean, random member-length errors on beam distortion. In that study, the length-averaged root-mean-square (rms) deflection of a single-layer truss beam of fixed length was found to have a minimum value that depends on the beam depth. In reference 3, an exact solution was presented for the standard deviation of nodal displacements in a 21-bay, free-free, statically determinate, single-layer truss beam with zero-mean, normally distributed member-length errors.

Since space applications require structural redundancy, there is a need to expand the analysis presented in references 2 and 3 to investigate statically indeterminate structures. To address that need, three types of truss beams were analyzed in the present paper: single layer, double layer, and modified double layer (double-layer beam with some members removed from one of the layers). The three beam types are illustrated in figure 1. The two different double-layer beams were employed to investigate the correlation between the extent of structural redundancy and the resulting surface error reduction.

The primary purpose of this study was to identify the geometric parameters that influence the rms surface error of truss beams containing randomly distributed member-length errors and to quantify their influence. Truss beams with pseudorandom length errors imposed on the members were analyzed using the EAL finite-element code (ref. 4). The rms surface error for a beam was calculated in terms of the normal distance from each upper surface node to a regression line for those nodes. Multiple rms surface error analyses were performed on nominally identical beams to produce the surface error statistics. For an example of the Monte Carlo approach to the study of surface error in doubly curved trusses, see reference 5.

Results for single-layer, double-layer, and modified double-layer beams are presented in the form of graphs of average rms surface error as a function of either beam length or beam depth. In addition, information on the scatter in rms surface error is presented, along with some information on the residual strut forces in the statically indeterminate double-layer and modified double-layer truss beams.

Symbols

A	strut cross-sectional area
D	beam depth
E	Young's modulus
L	truss beam length
ℓ	nominal strut length
N	number of struts in a truss beam
W	normal displacement of a node relative to a regression line
ϵ	strain
σ	standard deviation
$< >$	indicates average value over the beam length

A bar over a quantity indicates arithmetic mean.

Analysis

Truss Beam Models

The geometries of the three types of planar truss beams are shown in figure 1. The lower layer of the double-layer beam is simply the mirror image of the upper layer after the removal of two core members, or struts, from each end. The modified double-layer beam is derived by removing alternate pairs of diagonal struts from the lower layer of the double-layer beam. Pin-ended joints are assumed throughout all the beams. Also shown in figure 1 are formulas for the total number of struts in each beam as a function of the ratio of beam length, L, to strut length, ℓ. Table I contains a list of member properties, some of which are taken from reference 6. The tubular graphite/epoxy struts were assumed to have a nominal length of 2 m and a diameter of 2.54 cm and are typical of those considered in some envisioned applications. (See, for example, ref. 1.)

Strut Length Errors

The factors most likely to cause variability in the nominal length of a composite strut are manufacturing errors and uncertainties in the coefficient of thermal expansion. On the assumption of careful manufacturing practices and the use of material property data contained in reference 6, the uncertainties from these and all other sources were judged to be approximately equivalent to a length tolerance of ± 0.00254 cm (± 0.001 in.) for a 2-m-long strut. This length tolerance was taken as 2σ for the assumed zero-mean, standard normal distribution of member-length errors. Consistent with the analysis of reference 2, member-length errors were assumed to be proportional to member length; hence, they were treated as error strains. However, on the assumption that errors greater than 2σ would be detected during careful inspection, the corresponding "tails" of the normal distribution were cut off before length errors were assigned to the various members. The pseudorandom member-length errors were generated by use of a commercially available computer library routine.

Finite-Element Modeling

The finite-element program EAL (ref. 4) was employed to analyze the distorted truss beams. All the beams were composed of rod elements with pinned joints and were simply supported at the lower end nodes. The pseudorandom member-length errors were imposed on the individual struts as thermal strains, and the resulting computed nodal displacements were used in the calculation of surface error, as well as of the residual strut forces in the statically indeterminate beams. Two geometric parameters were varied independently to determine their influence on the rms surface error of the truss beams. While the length parameter was varied, the beam depth was held constant, and while the beam depth was varied, the beam length was held constant. Similar parametric studies were carried out on all three types of truss beams.

Best-Fit Surface Error Calculations

Root-mean-square surface error, W_{rms}, was defined in terms of the normal distance from a reference line to the upper surface nodes of the distorted beam. For comparison with results from reference 2 for simply supported beams, the reference line simply joined the upper surface nodes at each end of the beam. For free-free beam comparisons, the reference line was a least-squares best-fit line (regression line) for all upper surface nodes (see fig. 2). With the displacement of the ith node normal to the reference line denoted by W_i, the rms displacement is given by

$$W_{\text{rms}} = \sqrt{\frac{1}{N-1}\sum_{i=1}^{N} W_i^2}$$

where N is the number of surface nodes.

A set of 500 W_{rms} analyses (runs) was executed for each combination of values for L/ℓ and D/ℓ. The average W_{rms} value for each set of 500 runs was calculated from

$$\overline{W_{\text{rms}}} = \frac{1}{500}\sum_{j=1}^{500} W_{\text{rms},j}$$

The standard deviation of nodal displacement was obtained from

$$\sigma_W = \sqrt{\frac{1}{499}\sum_{j=1}^{500}(W_j - \overline{W})^2}$$

where $\overline{W}$ is the mean value of W_j from a set of 500 runs. In addition, the standard deviation of the W_{rms} values, σ_W, was computed for each set of 500 runs to obtain a measure of the scatter in W_{rms}.

Results and Discussion

Some information on the performance of the Monte Carlo approach in this study is given in table II. Five different seeds were chosen arbitrarily and supplied to the random number generator. The resulting pseudorandom numbers were used to calculate 500 W_{rms} values for a truss beam with $L/\ell = 20$ and $D/\ell = \sqrt{3}/2$. The cumulative average, $\overline{W_{\text{rms}}}$, of these values after 100, 300, and 500 runs is listed

in table II along with the corresponding seeds. For the five seeds, the difference between $\overline{W_{\text{rms}}}$ results after 100 runs and those after 500 runs ranges from 1.2 percent to 10.3 percent. The 10.3-percent change in $\overline{W_{\text{rms}}}$ for the last seed may suggest some sensitivity of the random number generator to the choice of seed. However, the sample of five values in table II is too small to support any strong conclusions. In the following, all the $\overline{W_{\text{rms}}}$ results have been nondimensionalized by $L\sigma_\epsilon$, where L is the total length of the beam, and σ_ϵ is the standard deviation of the truncated normal distribution of length-error strains. Each of the $\overline{W_{\text{rms}}}$ values was computed from 500 runs.

Single-Layer Beams

Figure 3 contains a graph of $\overline{W_{\text{rms}}}/L\sigma_\epsilon$ for a single-layer beam of fixed depth ratio $D/\ell = \sqrt{3}/2$ whose length ratio L/ℓ ranges from 10 to 100. Also shown is a plot of $(\overline{W_{\text{rms}}} + \sigma_W)/L\sigma_\epsilon$, where σ_W is the standard deviation of the 500 W_{rms} values. The increase in $\overline{W_{\text{rms}}}$ with an increase in the length ratio is due primarily to the increase in the number of surface members, whose errors promote beam curvature. Although the number of core members also increases, errors in their length cause a shear deformation that has a relatively small effect in a long beam. The $(\overline{W_{\text{rms}}} + \sigma_W)/L\sigma_\epsilon$ curve, which is approximately 50 percent higher than the $\overline{W_{\text{rms}}}/L\sigma_\epsilon$ curve, gives an indication of the scatter among the 500 W_{rms} values.

Figure 4 contains a graph of $\overline{W_{\text{rms}}}/L\sigma_\epsilon$ for a single-layer truss beam with $L/\ell = 40$ and with depth ratio D/ℓ ranging from $\sqrt{3}/2$ to 5. In this case the number of members remains constant; therefore, only the length ratio of surface members to core members affects $\overline{W_{\text{rms}}}$. The minimum $\overline{W_{\text{rms}}}$ point is approximately at $D/\ell = 2.75$. Small values of D/ℓ cause relatively large values of $\overline{W_{\text{rms}}}$ because surface members, which become long relative to core members, contribute primarily to beam curvature. As D/ℓ increases beyond 2.75, $\overline{W_{\text{rms}}}$ increases only gradually because core members, which become long relative to surface members, contribute to shear-type deformation rather than beam curvature. The shear-type deformation has a less profound effect than beam curvature on overall deflection. The $(\overline{W_{\text{rms}}} + \sigma_W)/L\sigma_\epsilon$ curve is approximately 40 percent above the curve for $\overline{W_{\text{rms}}}/L\sigma_\epsilon$ at the minimum point.

Figure 5 presents a comparison of results for single-layer beams of fixed depth ratio $D/\ell = \sqrt{3}/2$ with length ratio L/ℓ ranging from 3 to 100. The curve from reference 2 represents the exact solution for the length-averaged mean-square nodal displacement of a single-layer simply supported truss beam (assumed to have many members, thus modeled as a continuous uniform beam) with normally distributed random member-length errors. The curve from the present study is for pseudorandom member-length errors with a $\pm 2\sigma$-bounded normal distribution. The comparison between the present results and those of reference 2 shows good agreement, indicating that truncation of the length-error distribution in the present calculations was of little consequence.

Figure 6 presents a comparison of results from reference 3 and from the present study for a single-layer truss beam with $D/\ell = \sqrt{3}/2$ and $L/\ell = 21$. The result from reference 3 is the exact solution for rms surface nodal displacement of the truss beam with normally distributed random member-length errors. Agreement between the present results and those of reference 3 is good. Small differences between the two are probably due, in part, to the fact that the present calculations are based on the normal distance from the best-fit line to the nodes, while those in reference 3 are based on vertical distance.

Double-Layer Beams

Figure 7 contains a graph of $\overline{W_{\text{rms}}}/L\sigma_\epsilon$ for a double-layer truss beam with $D/\ell = \sqrt{3}$ and L/ℓ ranging from 20 to 100. This truss beam is twice as deep as the single-layer truss beam. Since this beam is statically indeterminate, member-length errors give rise to internal forces. The trend shown in figure 7 is similar to that for the single-layer beam (fig. 3), where $\overline{W_{\text{rms}}}$ increases because the growing number of surface members causes greater beam curvature. The $(\overline{W_{\text{rms}}} + \sigma_W)/L\sigma_\epsilon$ curve on this graph is approximately 50 percent above the mean curve.

Figure 8 contains a graph of $\overline{W_{\text{rms}}}/L\sigma_\epsilon$ for a double-layer truss beam with $L/\ell = 40$ and D/ℓ ranging from $\sqrt{3}$ to 9. A minimum value of $\overline{W_{\text{rms}}}$ occurs approximately at $D/\ell = 4.5$. This behavior is similar to that for the single-layer truss beam (fig. 4), where small D/ℓ values promote beam curvature effects and large D/ℓ values promote shear-type deformation. The $(\overline{W_{\text{rms}}} + \sigma_W)/L\sigma_\epsilon$ curve is again approximately 40 percent above the $\overline{W_{\text{rms}}}/L\sigma_\epsilon$ curve at the minimum point.

Modified Double-Layer Beams

In figure 9, $\overline{W_{\text{rms}}}$ for a modified double-layer truss beam with $D/\ell = \sqrt{3}$ is plotted as a function of L/ℓ, which ranges from 20 to 100. Alternating pairs of core members have been removed, so that lower surface members are twice as long as upper surface members. The trend is similar to that in figures 3 and 7, where $\overline{W_{\text{rms}}}$ increases steadily with L/ℓ. The $(\overline{W_{\text{rms}}} + \sigma_W)/L\sigma_\epsilon$ curve is approximately 50 percent above the $\overline{W_{\text{rms}}}/L\sigma_\epsilon$ curve.

Figure 10 contains a graph of $\overline{W_{\text{rms}}}/L\sigma_\epsilon$ for a modified double-layer truss beam with $L/\ell = 40$, and with D/ℓ ranging from $\sqrt{3}$ to 9. A minimum $\overline{W_{\text{rms}}}$ point was achieved approximately at $D/\ell = 4$. This result is similar to those in figures 4 and 8 for the single-layer and double-layer beams, where smaller D/ℓ values increase $\overline{W_{\text{rms}}}$ by promoting beam curvature effects, while larger D/ℓ values increase $\overline{W_{\text{rms}}}$ primarily because of shear-type deformation. As before, the $(\overline{W_{\text{rms}}} + \sigma_W)/L\sigma_\epsilon$ curve is approximately 40 percent above the mean curve at the minimum point.

Comparison of Beam Types

Figure 11 contains graphs of $\overline{W_{\text{rms}}}/L\sigma_\epsilon$ for the three types of truss beams with $D/\ell = \sqrt{3}$ and L/ℓ ranging from 20 to 100. Note that the depth of this single-layer truss beam is twice that of the single-layer beam in figure 3. For this value of D/ℓ, there is little difference between the single-layer and double-layer beam results. Furthermore, $\overline{W_{\text{rms}}}$ is actually greater in the modified double-layer beam than in the single-layer beam. Considered alone, this result could lead to an erroneous conclusion about the effects of structural redundancy on rms error.

A clearer perspective on this issue is provided by figure 12, where graphs are shown of the minimum $\overline{W_{\text{rms}}}$ values for the three types of truss beams with $L/\ell = 40$ and D/ℓ ranging from $\sqrt{3}$ to 9. The minimum $\overline{W_{\text{rms}}}$ value for the modified double-layer beam is approximately 16 percent lower than that for the single-layer beam. This modest improvement is achieved with a 37-percent increase in the number of struts. The full double-layer beam achieves a 35-percent reduction in $\overline{W_{\text{rms}}}$ with a corresponding 73-percent increase in the number of struts. Therefore, both double-layer beams are capable of greater surface accuracy than that of the single-layer beam. However, on the basis of strut count alone, both double-layer beams appear less attractive in comparison with the single-layer beam. Of course, in addition to surface accuracy and strut count, a beam design for a particular application would likely be impacted by other considerations, for example, number of joints, manufacturing and construction costs, and assembly time.

Residual Strut Forces

In addition to rms surface errors, member axial forces in the statically indeterminate double-layer beam were calculated for $L/\ell = 40$ and eight values of D/ℓ ranging from $\sqrt{3}$ to 9. The largest calculated member force was 173 N, and the average of the maximum values from each of the eight analyses was 164 N. As a rough estimate of the likelihood of member buckling due to residual forces, the largest member force was compared with the Euler buckling load for the longest member in the optimum double beam ($D/\ell = 4.5$) with simple supports assumed. The largest member force was found to be about 28 percent of the Euler load, a result which indicates that member buckling due to residual forces in the optimum beam would be quite unlikely for the range of member-length errors assumed here. Of course, the residual strut forces give rise to other considerations, such as joint preload and creep in bonded joints, which are outside the scope of the present report.

Concluding Remarks

A Monte Carlo approach combined with finite-element analysis has been used to calculate surface-error statistics for three types of truss beams distorted by pseudorandom member-length errors. One beam was a single-layer, statically determinate structure, while the other two were variations of a statically indeterminate double-layer design. Length and depth parameters were varied independently to assess their influence on the surface error of truss beams. For beams of fixed depth, the rms surface error was seen to increase steadily with beam length. However, beams of fixed length were found to have a depth at which rms surface error was a minimum. In general, the statically indeterminate double-layer beams showed potential for greater surface accuracy, though at the expense of a disproportionately greater number of struts. For example, the full double-layer beam of optimum depth employed 73 percent more struts than the single-layer beam to achieve a 35-percent reduction in rms surface error. Also, limited calculations of member axial forces in some statically indeterminate beams indicate that member buckling due to residual forces would be quite unlikely for the range of member-length errors considered.

NASA Langley Research Center
Hampton, VA 23665-5225
January 12, 1990

References

1. Hedgepeth, John M.; and Miller, Richard K.: *Structural Concepts for Large Solar Concentrators.* NASA CR-4075, 1987.
2. Hedgepeth, John M.: Accuracy Potentials for Large Space Antenna Structures. *39th Annual Conference of the Society of Allied Weight Engineers, Inc.*, May 1980, Paper No. 1375.

3. Burdisso, Ricardo A.; and Haftka, Raphael T.: Optimal Location of Actuators for Correcting Distortions in Large Truss Structures. *AIAA J.*, vol. 27, no. 10, Oct. 1989, pp. 1406–1411.
4. Whetstone, W. D.: *EISI-EAL Engineering Analysis Language Reference Manual—EISI-EAL System Level 2091. Volume 2: Structural Analysis—Primary Processors.* Engineering Information Systems, Inc., July 1983.
5. Greene, William H.: Effects of Random Member Length Errors on the Accuracy and Internal Loads of Truss Antennas. *J. Spacecr. & Rockets,* vol. 22, no. 5, Sept.–Oct. 1985, pp. 554–559.
6. Johnson, Robert R.; Kural, Murat H.; and Mackey, George B.: *Thermal Expansion Properties of Composite Materials.* NASA CR-165632, 1981.

Table I. Truss-Member Properties

Cross-sectional area, A, cm^2 (in^2)	1.14	(0.18)
Member diameter, cm (in.)	2.54	(1)
Member wall thickness, cm (in.)	15	(0.06)
Nominal member length, ℓ, cm (in.)	200	(78.74)
Coefficient of thermal expansion, per °C (per °F)	0.18×10^{-6}	(0.1×10^{-6})
Young's modulus, E, N/cm^2 (lb/in^2)	20.68×10^6	(30×10^6)

Table II. Statistical Study of Monte Carlo Technique

Seed	$\overline{W_{rms}}$			Variation between 100 and 500 runs, percent
	100 runs	300 runs	500 runs	
27 712	0.00872	0.00858	0.00862	1.2
222 222	.00908	.00905	.00893	1.7
111 111	.00928	.00899	.00891	4.2
191 919	.00918	.00878	.00875	4.9
876 374	.00933	.00883	.00846	10.3
Average.	0.00912	0.00885	0.00873	
Variation about average, percent.	−4.6 to 2.3	−3.2 to 2.3	−3.2 to 2.2	

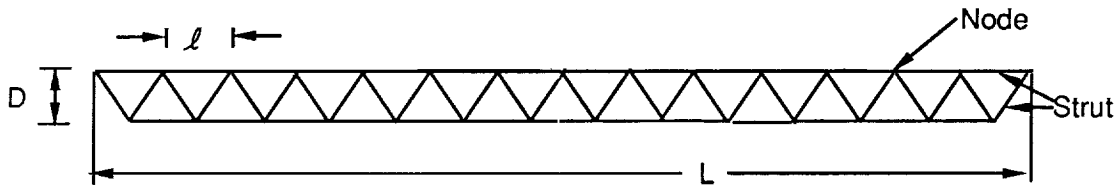

$$N_{struts} = 4\frac{L}{\ell} - 1, \frac{L}{\ell} \geq 1$$

Single-layer

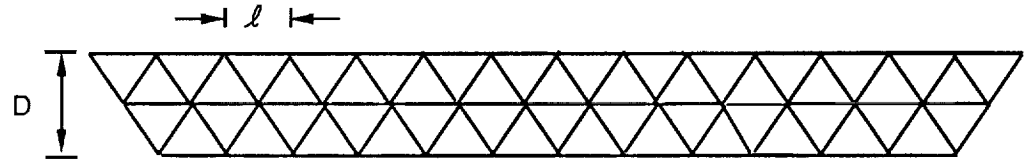

$$N_{struts} = 7\frac{L}{\ell} - 1, \frac{L}{\ell} \geq 2$$

Double-layer

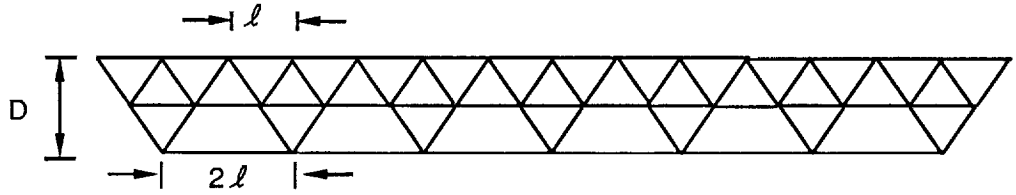

$$N_{struts} = \frac{11}{2}\frac{L}{\ell} - 2, \frac{L}{\ell} \geq 4, \text{even}$$

Modified double-layer

Figure 1. Sketch of three types of truss beams.

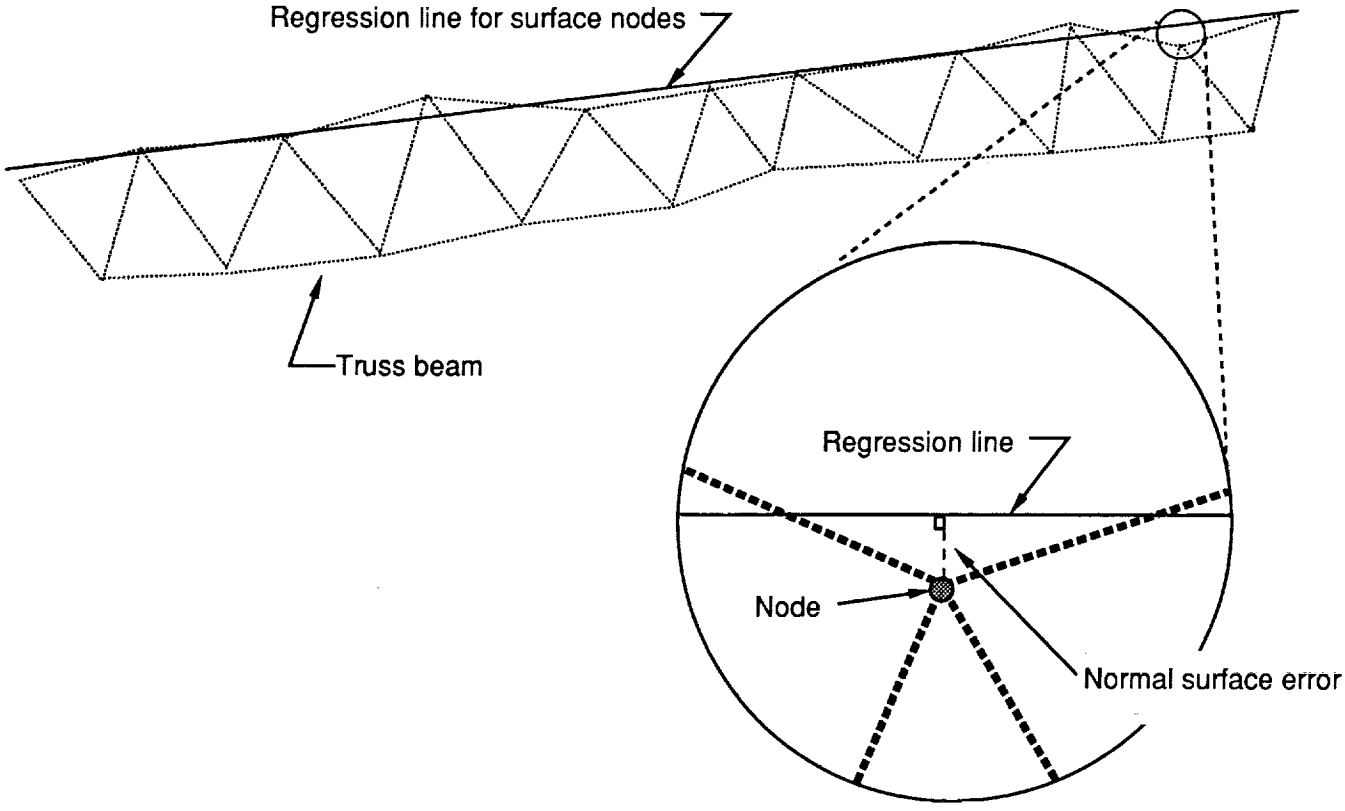

Figure 2. Illustration of effect of manufacturing length errors on truss beams.

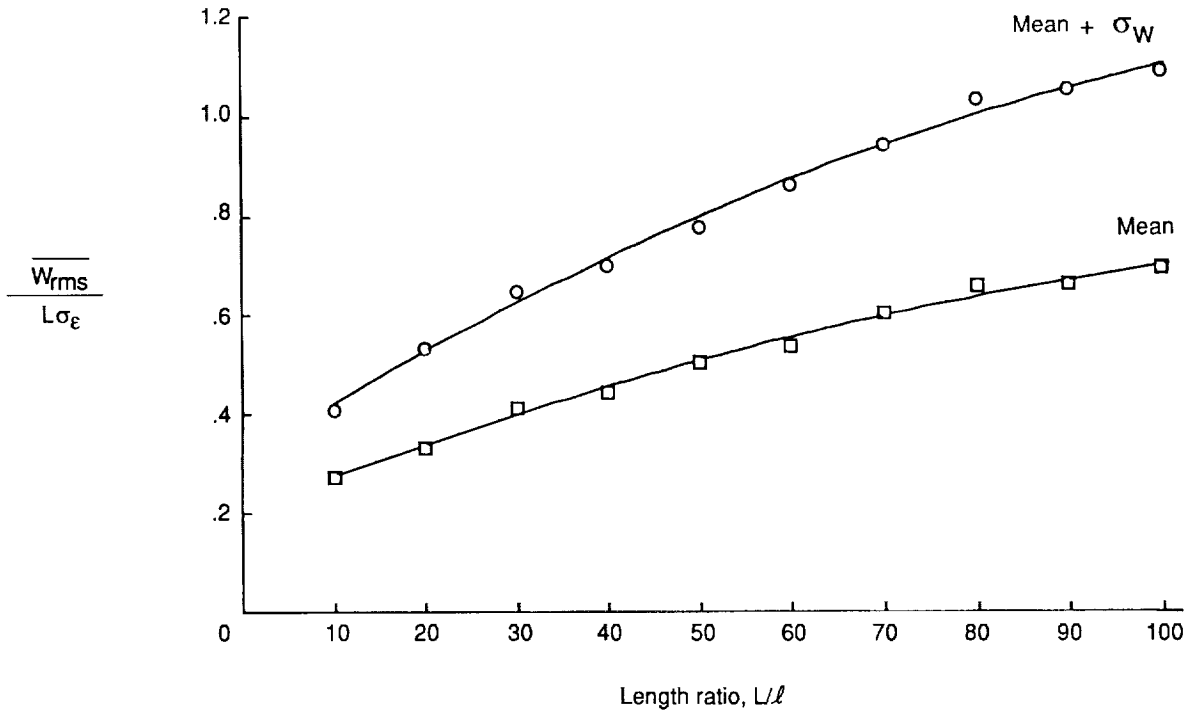

Figure 3. Effect of length of single-layer constant-depth truss beams on rms error. $D/\ell = \sqrt{3}/2$.

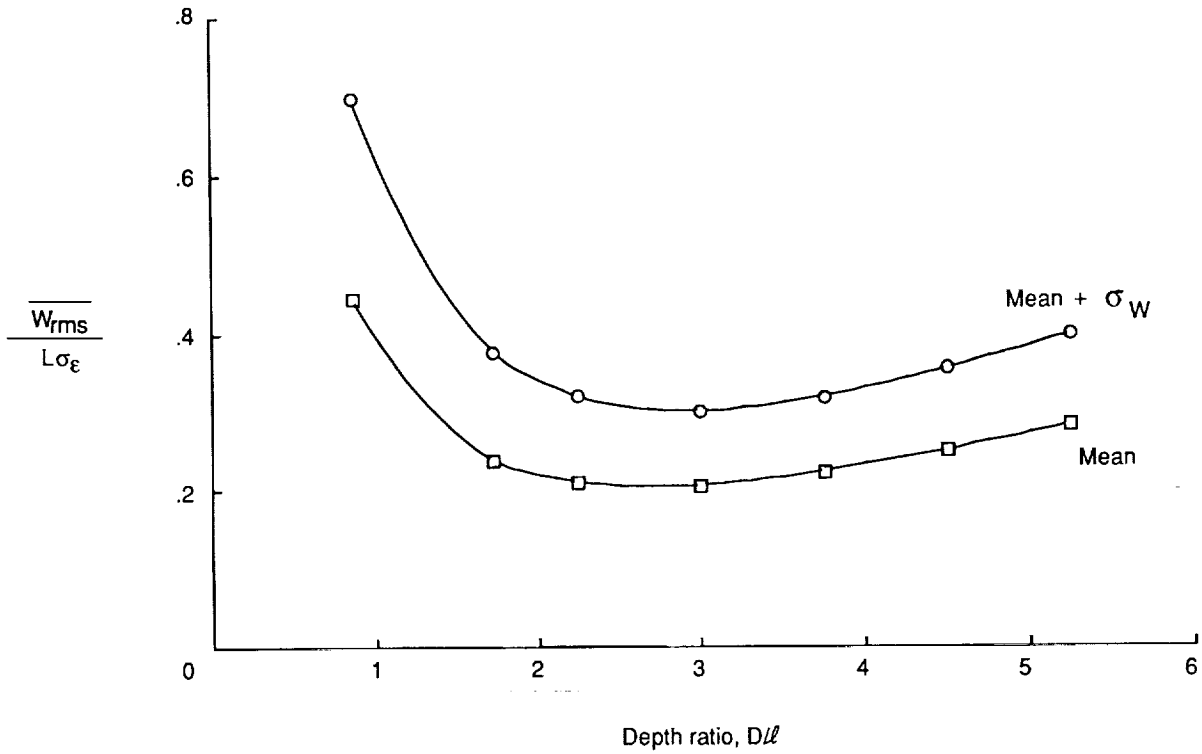

Figure 4. Effect of depth of single-layer truss beam on rms error. $L/\ell = 40$.

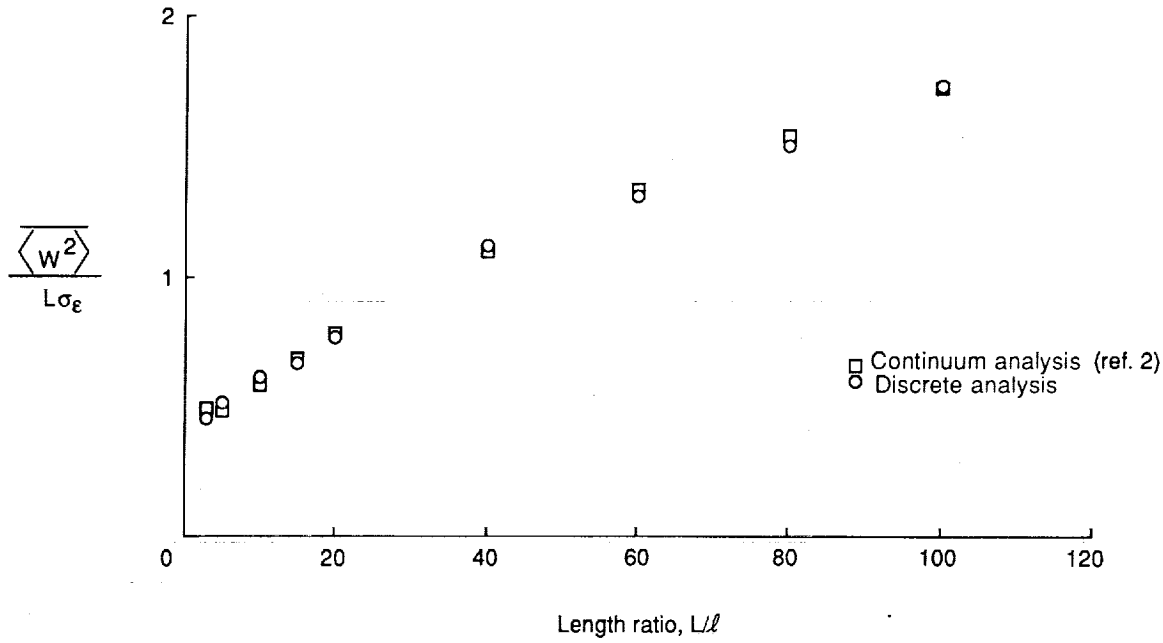

Figure 5. Effect of length of single-layer constant-depth truss beams on the length-averaged mean-squared displacement. $D/\ell = \sqrt{3}/2$.

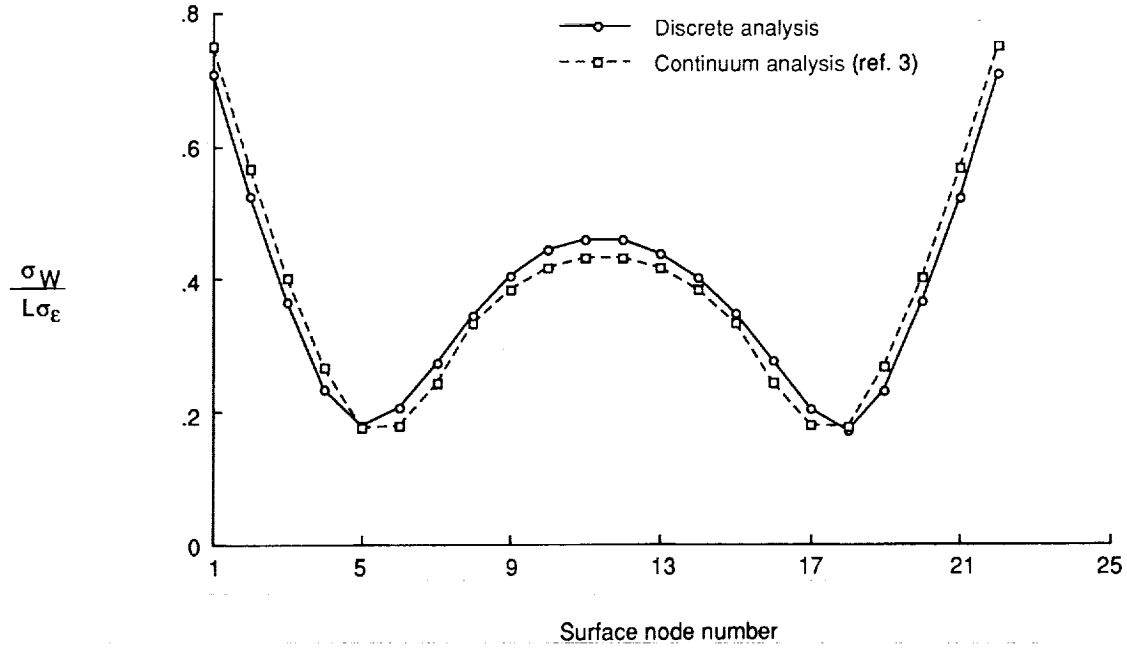

Figure 6. Standard deviation of nodal displacement for a free-free single-layer beam. $D/\ell = \sqrt{3}/2$.

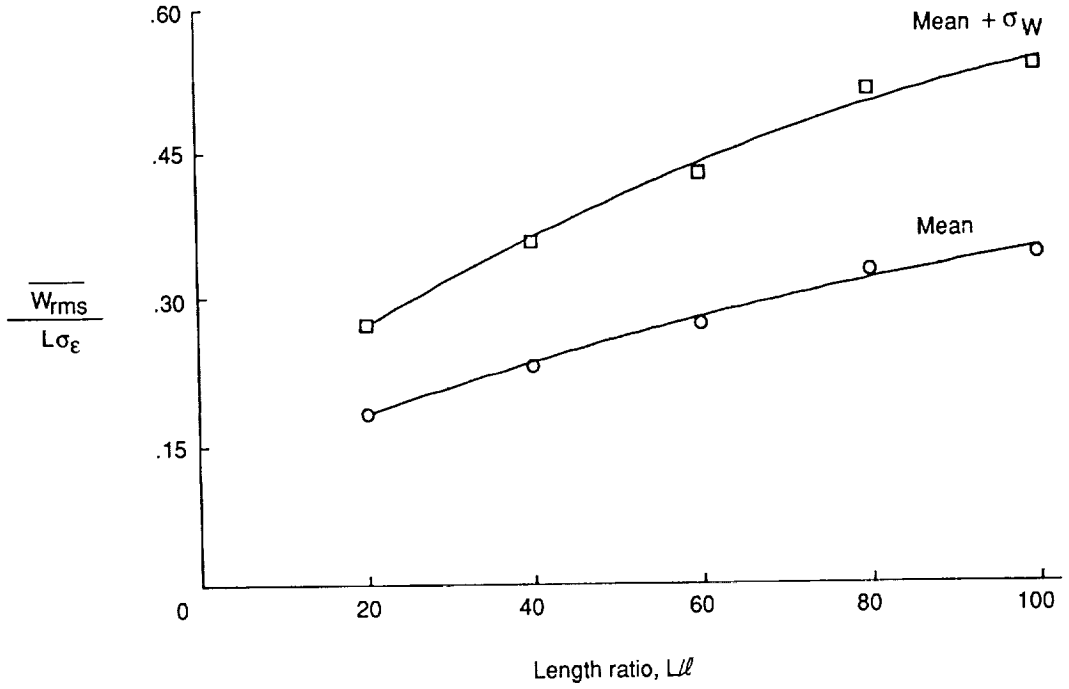

Figure 7. Effect of length of double-layer constant-depth truss beams on rms error. $D/\ell = \sqrt{3}$.

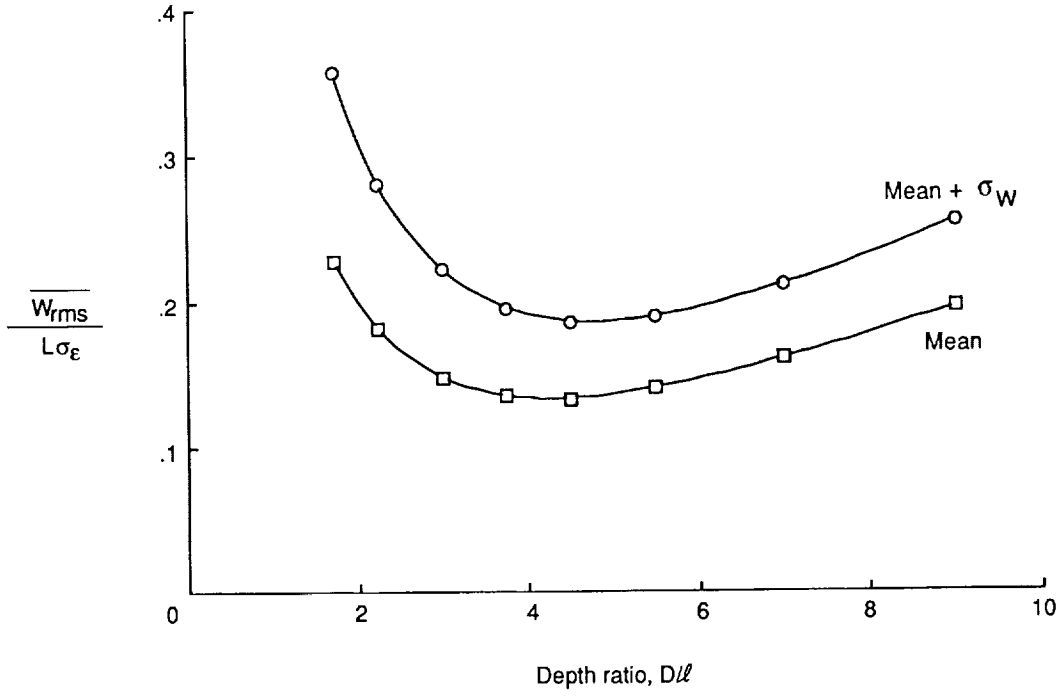

Figure 8. Effect of depth of double-layer truss beam on rms error. $L/\ell = 40$.

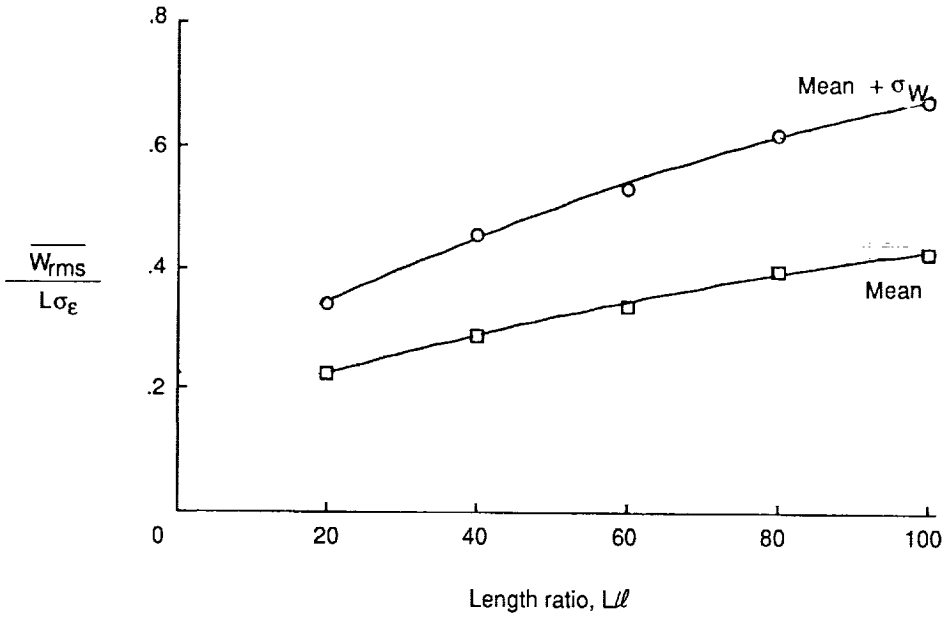

Figure 9. Effect of length of modified double-layer constant-depth truss beam on rms error. $D/\ell = \sqrt{3}$.

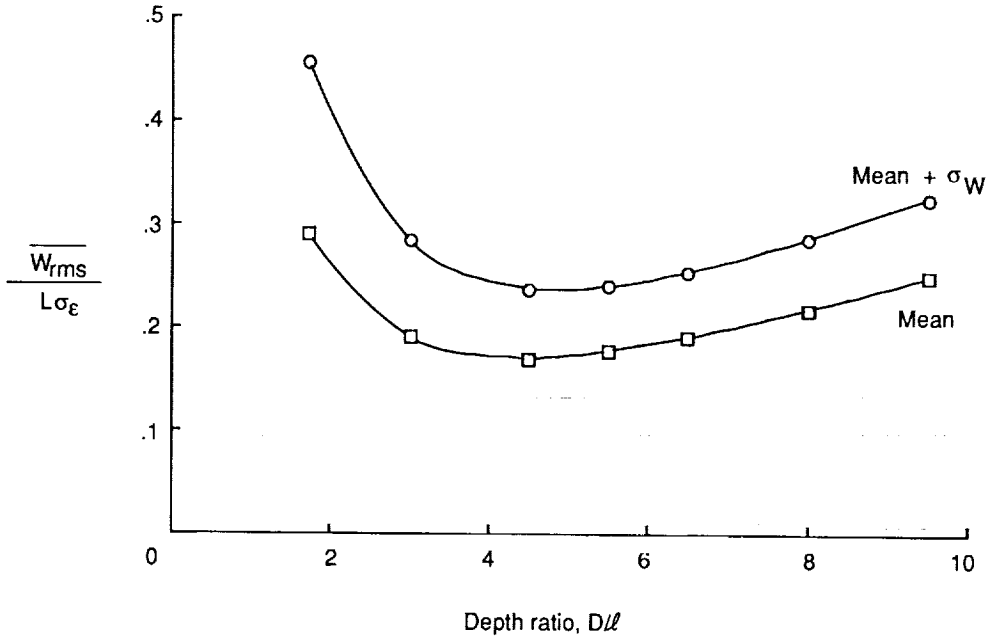

Figure 10. Effect of depth of modified double-layer truss beam on rms error. $L/\ell = 40$.

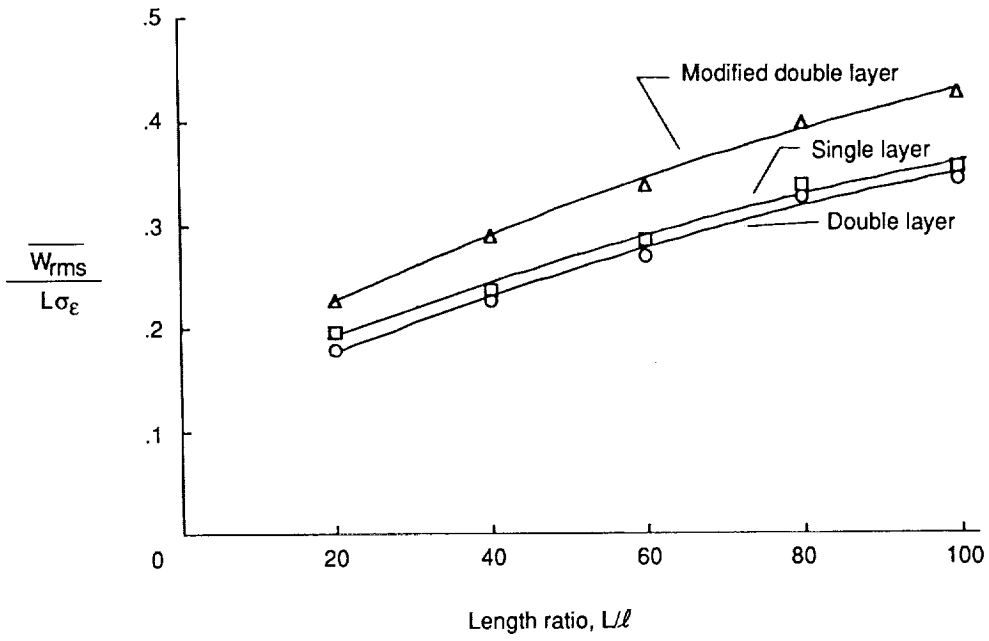

Figure 11. Effect of length of three truss beams of equal depth on rms error. $D/\ell = \sqrt{3}$.

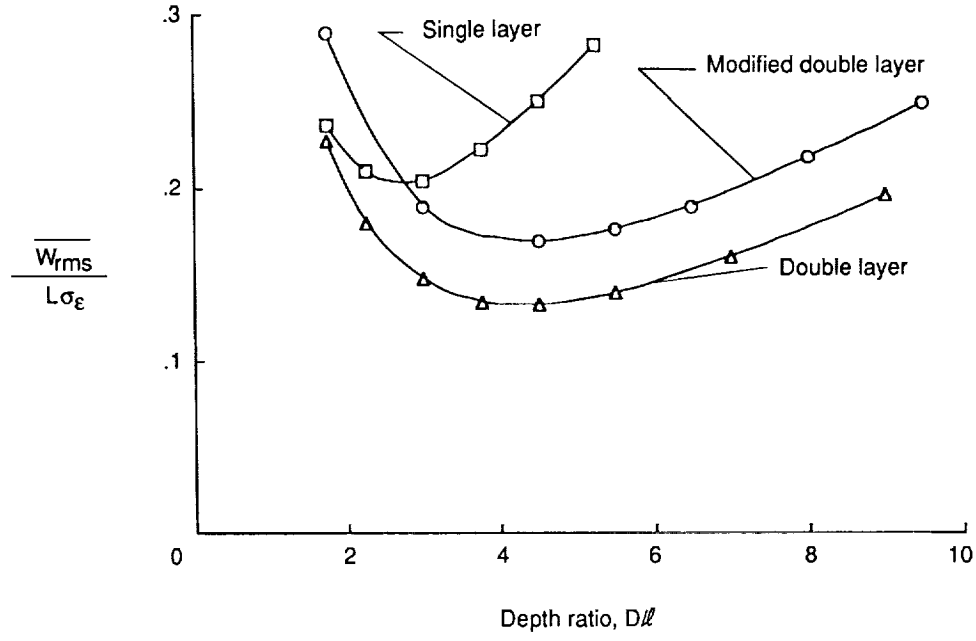

Figure 12. Effect of depth of three truss beams on rms error. $L/\ell = 40$.

NASA
National Aeronautics and Space Administration

Report Documentation Page

1. Report No.	2. Government Accession No.	3. Recipient's Catalog No.
NASA TM-4161		

4. Title and Subtitle	5. Report Date
A Statistical Study of the Surface Accuracy of a Planar Truss Beam	February 1990
	6. Performing Organization Code
7. Author(s)	8. Performing Organization Report No.
W. Scott Kenner and W. B. Fichter	L-16656
9. Performing Organization Name and Address	10. Work Unit No.
NASA Langley Research Center Hampton, VA 23665-5225	506-43-41-02
	11. Contract or Grant No.
12. Sponsoring Agency Name and Address	13. Type of Report and Period Covered
National Aeronautics and Space Administration Washington, DC 20546-0001	Technical Memorandum
	14. Sponsoring Agency Code

15. Supplementary Notes

16. Abstract

Surface error statistics for single-layer and double-layer planar truss beams with random member-length errors were calculated using a Monte Carlo technique in conjunction with finite-element analysis. Surface error was calculated in terms of the normal distance from a regression line to the surface nodes of the distorted beam. Results for both single-layer and double-layer beams indicate that a minimum root-mean-square surface error can be achieved by optimizing the depth-to-length ratio of a truss beam. The statically indeterminate double-layer beams can provide greater surface accuracy, though at the expense of significantly greater complexity.

17. Key Words (Suggested by Authors(s))	18. Distribution Statement
Surface error Planar truss beam Monte Carlo technique	Unclassified—Unlimited Subject Category 39

19. Security Classif. (of this report)	20. Security Classif. (of this page)	21. No. of Pages	22. Price
Unclassified	Unclassified	14	A03

For sale by the National Technical Information Service, Springfield, Virginia 22161-2171